Mass Transfer in a Liquid-Liquid CFSTR

The performance of a two-phase liquid-liquid continuous flow stirred tank reactor (CFSTR) was evaluated experimentally by simultaneous determination of dispersed phase drop size distribution and extraction efficiency as a function of reactor operating conditions. The results provided a basis against which predictions made by a previously developed simulation technique (Bapat et al., 1984) were compared. The close agreement between the experimental and the simulation results validates the drop rate models and the simulation algorithm employed in this work.

P. M. BAPAT
Department of Chemical Engineering
Illinois Institute of Technology
Chicago, IL 60616

and L. L. TAVLARIDES
Department of Chemical Engineering and
Materials Science
Syracuse University
Syracuse, NY 13210

SCOPE

Multiphase contacting is a commonly used operation in chemical process industries handling a wide range of substances in different forms and states of matter. Two-phase liquid-liquid contacting, which is a major multiphase operation, is frequently encountered in nuclear, hydrometallurgical, petrochemical, pharmaceutical, and food industries for extracting valuable substances. The optimum design and operation of such an extraction system require, in addition to the homogeneous reaction kinetics, a thorough understanding of the physical rate processes. The physical factors which influence the extractor performance are: (1) dispersed phase droplet processes (breakage and coalescence); (2) microscopic interphase transport processes; and (3) macroscopic flow patterns in the contacting equipment.

The effect of these individual factors and their mutual interaction has not yet been quantitatively formulated by a comprehensive model. As a step in that direction, this work investigates the first two factors for a homogeneous liquid-liquid dispersion in a continuous flow stirred tank reactor (CFSTR). The dynamics of the dispersed phase drop interactions and the microscopic interphase mass transfer in the turbulent flow field were simulated to predict the behavior of the liquid extractor. The predictions are validated by comparison against the experimental data acquired from a cyclohexane/carbontetrachloride(d)-[iodine]-water(c) dispersion agitated in a one-liter CFSTR system capable of providing simultaneous determination of drop size distribution and extraction efficiency. The drop size distributions are obtained by in situ photomicrography. The mass transfer efficiencies are estimated by spectrophotometric iodine concentration measurements of the reactor dispersion phases separated by a specially developed instantaneous in situ membrane filtration technique.

In the past, the population balance equation (PBE) that provides the mathematical apparatus for describing the particulate systems has been used successfully to obtain the dispersion state distributions (Valentas and Amundson, 1966; Bayens and Laurence, 1969; Bajpai et al., 1976; Coulaloglou and Tavlarides, 1977). The complexity of numerically solving the integrodifferential PBE is bypassed by resorting to simulation techniques. Spielman and Levenspiel (1965) and Shah et al. (1977) simulated a CFSTR using Curl's (1963) model. The dispersion under turbulent hydrodynamics, however, is too complex to be adequately represented by the Curl's model. Hsia and Tavlarides (1980, 1983) made significant progress in this direction by using realistic drop interaction functions based on Coulaloglou's (1975) models. Recent refinements in the time management techniques of a simulation algorithm developed by Bapat et al. (1984) have been used in the present work.

Simulation of interphase transport in two-phase liquid-liquid dispersions has not been successfully attempted before the present work. The highly interactive droplet swarm in a turbulent environment has precluded any theoretical treatment of these processes. Experimental estimation of interphase mass transfer also encounters major difficulties due to turbulence in mechanically agitated stirred tanks. Because the mass transfer efficiencies in stirred tanks are high, the experimental estimation techniques need to be very accurate. This problem is compounded by the fact that the solute concentration cannot be measured easily in a single phase of the turbulently agitated dispersion. The paucity of data in this area reflects these difficulties.

CONCLUSIONS AND SIGNIFICANCE

A simulation procedure developed previously (Bapat et al., 1984) is shown to be capable of accurately predicting extraction mass transfer data by considering the effects of dispersion drop size distribution and reactor power dissipation on microscopic interphase transport. The major improvements of this simulation algorithm included realistic drop interaction functions based on hydrodynamic considerations and an efficient system for managing simulation time by the method of interval of quiescence.

A specially designed one-liter CFSTR system was constructed to obtain data to test the simulation procedure. The system is capable of simultaneous determination of mass transfer efficiency and the drop size distribution. A new experimental

---

P. M. Bapat is presently at Goodyear Tire and Rubber, Akron, OH 44316.

technique made it possible to monitor accurately interphase solute transfer. The range of experimental conditions was as follows: power dissipation per unit mass, (0.155, 0.906) m^2/s^3; residence time, (60, 120) s; dispersed phase fraction, (0.05, 0.15); solute feed concentration: organic phase, $(1 \times 10^{-3}, 3 \times 10^{-3})$ M (mol/m^3) and aqueous phase, $(1 \times 10^{-4}, 2 \times 10^{-4})$ M. The experimental and the simulated CFSTR results agree very well. The average deviations between the predicted and the experimental values for Sauter mean diameters and extraction efficiencies are ±5.0% and ±3.4%, respectively. Both the experimental system and the simulation algorithm can be easily extended to investigate extraction in reactive dispersions.

It is observed that the increased collision frequencies and the turbulence damping arising from the increased dispersed phase fraction cause an increase in the average drop size of the dispersed phase. The resulting enhancement in drop micromixing also causes an increase in the extraction efficiency. The experimental data confirm the effect of interphase mass transfer of a solute with a negative interfacial tension gradient on the dispersion drop size. Transfer of iodine from the dispersed to the continuous phase resulted in increased coalescence with a subsequent increase in drop size and decrease in extraction efficiency. This experimental work has also demonstrated the unsuitability of a weakly surface-active solute such as iodine to investigate the effect of concentration driving forces and mass transfer directions on extraction efficiencies.

INTRODUCTION

In a two-phase liquid-liquid operation, one liquid is dispersed into the other, thereby increasing interphase transport processes. Investigations of two-phase phenomena are generally focused on the spread of the dispersed phase droplet properties. The characterization of the distribution of the dispersed phase with respect to its property vector ($\bar{x}$) is formalized by the drop population balance equations. Following Randolph and Larson (1971), the dispersed phase droplet number continuity equation in its most general form can be written as

$$\frac{\delta n}{\delta t} + \nabla \cdot (\dot{\bar{x}} n) - B + D = 0. \qquad (1)$$

The birth B and death D functions involve integral expressions with variable limits (Valentas and Amundson, 1966; Coulaloglou and Tavlarides, 1977) and thus render the PBE a partial integrodifferential equation whose general analytical solution has not yet been found. The population balance equation (PBE) approach to obtain the state of the dispersion, although mathematically elegant, cannot be used analytically except in very simple cases (Ramkrishna, 1974; Bajpai et al., 1976). The numerical techniques employed to treat the realistic cases become increasingly unwieldy as the dimensionality of the dispersed phase space increases. Bayens and Laurence (1969) have pointed out that the intractability of the PBE derives chiefly from the terms involving time rate of change of an internal property such as the drop solute concentration.

Simulation methods offer an attractive alternative for obtaining the dispersion state by obviating the need for solving the involved multidimensional integrodifferential equations. The digital simulation techniques are therefore free of the troublesome mathematical convergence and stability problems usually associated with numerical algorithms. Since Spielman and Levenspiel's (1965) Monte Carlo simulation of chemical reactors, many other investigations have appeared in the literature (Zeitlin and Tavlarides, 1972; Jakubowsky and Sideman, 1876; Shah et al. 1977; Hsia and Tavlarides, 1980 and 1983). However, in most cases (with the exception of Hsia and Tavlarides), the drop rate functions have been represented by simplistic models. Jakubowsky and Sideman assumed constant coalescence frequency, while Shah and co-workers adopted Curl's model in which coalescence is instantaneously followed by a bisection to retain the monodispersed character of the drop population. Except for Shah and co-workers who used an interval of quiescence method, a time-oriented method of simulation time advancement was used by most workers. The artificial discretization of time increment renders the algorithm unsuitable for monitoring a continuous system such as the mechanical agitated liquid dispersion. The remedial measure of decreasing the size of the time increment to represent the continuous nature of the system makes the method computationally inefficient (Gordon, 1969). The algorithm used in the present work overcomes these two deficiencies by means of realistic drop rate functions derived from the hydrodynamic considerations together with an event-oriented technique based on the interval of quiescence method. The latter allows the evolution of the dispersion from its initial state to the final state in a smooth, natural manner without any arbitrary discretization of time.

SIMULATION MODEL

The evolution of the ensemble of drops to final steady state is marked by successive sample events separated from each other by an interval of quiescence, t_{IQ}. This interval is computed by the Poisson arrival pattern analysis (Graybeal and Pooch, 1980) as follows:

$$t_{IQ} = -\ln x/(f_b + f_c + f_e). \qquad (2)$$

The simulation algorithm calculates the interphase mass transfer between the individual drops of the sample and the continuous phase during this time interval. The transport process is treated as deterministic by appropriate balance equations. At the end of the interval of quiescence, a drop event is executed, and as a result the sample constituency is slightly changed. For example, if the drop exits from the CFSTR, the sample count decreases by 1 while the breakage of the drop increases the count by 1. In any event, the interactive nature of the coalescing drop population causes the coalescence frequencies of the individual drops to be altered. Therefore the simulation algorithm computes new individual drop and sample frequencies. The event cycle is repeated until the simulation pass time is completed. The drop dispersion statistics are computed at the conclusion of each pass and the results are displayed. The simulation continues until the steady state is attained. Details of the simulation algorithm are given elsewhere (Bapat, 1982; Bapat et al., 1984) and will not be repeated here.

Drop Rate Functions

In addition to the dispersed phase breakage and coalescence in a CFSTR, drops enter and leave the reactor to sustain the continuous flow operation. The success of the simulation algorithm in predicting the performance of the extractor depends upon the validity of the drop rate models used. The event frequency functions used in this work are described below.

Feed Frequency. The feed is considered to occur at regular intervals and is executed deterministically by maintaining a separate feed timer in the simulation algorithm. The feed frequency is calculated by the following formula:

$$f_f = (V_d/\tau)/v_f. \qquad (3)$$

The feed frequency does not appear in the interval of quiescence equation (Eq. 2) because of its deterministic nature. The feed frequency is maintained at a constant value throughout a simulation run.

Exit Frequency. The exit frequency of a drop is assumed to be independent of its properties. Therefore the total exit frequency of the sample is given by

$$f_e = N/\tau. \tag{4}$$

Breakage Frequency. Coulaloglou's (1975) expression for breakage frequency is used in this work.

$$g(a_i) = C_1 \frac{\epsilon^{1/3}}{(1 + \phi)a_i^{2/3}} \exp\left[-C_2 \frac{\sigma(1 + \phi)^2}{\rho_d \epsilon^{2/3} a_i^{5/3}}\right] \tag{5}$$

The total breakage frequency of the sample is given by

$$f_b = \sum_{i=1}^{N} g(a_i). \tag{6}$$

Breakage is assumed to be binary. The daughter droplet probability volume distribution is given by the β-distribution.

$$\beta(a_1;a_j) = 30(a_i^3/a_j^3)^2(1 - a_i^3/a_j^3)^2 \tag{7}$$

Coalescence Frequency. The frequency of a drop of diameter a_i coalescing with drop a_j is given by Coulaloglou (1975) as

$$F(a_i,a_j) = C_3 \frac{\epsilon^{1/3}}{1 + \phi}(a_i + a_j)^2(a_i^{2/3} + a_j^{2/3})^{1/2} \cdot \exp\left\{-C_4 \frac{\mu_c \rho_c \epsilon}{\sigma^2(1 + \phi)^3}\left(\frac{a_i a_j}{a_i + a_j}\right)^4\right]. \tag{8}$$

The coalescence frequency of a single drop of diameter a_i is given by

$$f_{c,a_i} = \sum_{\substack{j=1 \\ j \neq i}}^{N} F(a_i,a_j). \tag{9}$$

The total sample coalescence frequency is given by

$$f_c = 1/2 \sum_{i=1}^{N} \sum_{\substack{j=1 \\ j \neq i}}^{N} F(a_i,a_j). \tag{10}$$

Mass Transfer

The drop events considered above cause an abrupt change in the sample constituency because of an almost instantaneous change in the identity of the participating drop(s). In an extractive dispersion, however, the dispersed phase droplets continually undergo a smooth transition in their properties due to interphase transport processes which are adequately described by appropriate equations for conservation of mass and energy. The present simulation algorithm considers the isothermal interphase mass transfer of a single solute. Extension to a multicomponent system with or without chemical reaction is straightforward.

The solute mass balance for a drop of diameter a_i when the resistance to mass transfer lies predominantly in the continuous phase can be written as

$$-(\pi/6)a_i^3 \frac{dC_{d,i}}{dt} = k\pi a_i^2(C_{d,i}/\kappa - C_c)$$

and

$$C_{d,i} = C_{d,i}^* \text{ at } t = 0. \tag{11}$$

The quasi-steady state solution to the above equation gives the amount of solute transferred to the continuous phase in time t_{IQ} as

$$m_i = (\pi/6)a_i^3(C_{d,i}^* - \kappa C_c)\left[1 - \exp\left(-\frac{6Sh_i \mathcal{D}_c t_{IQ}}{\kappa a_i^2}\right)\right]. \tag{12}$$

The continuous phase concentration at the end of the interval of quiescence is given by a discretized species material balance in the continuous phase.

$$C_{c,2} = \left[V_c C_{c,1} + \sum_{i=1}^{N} m_i + (V_c/\tau)t_{IQ}(C_{c,f} - C_{c,1}\right] \Big/ V_c \tag{13}$$

where

$$V_c = [(1 - \phi)/\phi]V_d. \tag{14}$$

The mass transfer efficiency is calculated by the following equation:

$$E = (C_c - C_{c,f})/(C_{c,e} - C_{c,f}). \tag{15}$$

The equilibrium aqueous effluent concentration, $C_{c,e}$ is obtained by taking the solute balance over the entire CFSTR.

$$C_{c,e} = (Q_d C_{d,f} + Q_c C_{c,f})/(\kappa Q_d + Q_c) \tag{16}$$

The problem of estimating the mass transfer coefficients for liquid drops in a turbulent medium does not have a complete solution at present. For the potential flow ($Re \rightarrow \infty$), two cases are considered in the literature. For a clean liquid drop having a mobile interface ($u/U = 3/2$), the average Sherwood number is given as (Boussnesq, 1905)

$$Sh = (4/\pi)^{1/2} Re^{1/2} Sc^{1/2}. \tag{17}$$

At the other extreme, when the drop interface is immobile ($u/U = 0$), the mass transfer through the boundary layer is represented by an equation of the form

$$Sh = K\, Re^{1/2} Sc^{1/3}.\ 0.5 < K < 1.0 \tag{18}$$

Skelland's detailed review (1974) of the forced convection mass transfer from single spheres provides tabulated equations giving values of K and the range of applicability.

The mass transfer of a solute in a ternary dispersion changes the concentration of the dispersed phase drops as time advances. The solute transfer in time makes the process inherently unsteady. Ruckenstein (1967, 1968) used the penetration theory to analyze this problem, but the derived relationships are extremely cumbersome. Clift et al. (1978) have provided simplified solutions accurate to within ±3%. The variation of mass transfer coefficient with time renders these equations of little value in actual design calculations. Dang et al. (1970) examined the conditions under which the quasi-steady state assumption (used in obtaining the solution of Eq. 11) can be made when the mass transfer resistance resides mainly in the continuous phase. The conditions are

Quasisteady State Assumption:

$$\kappa\, Pe^{1/2} \gg 1. \tag{19}$$

Localization of Mass Transfer Resistance to the Continuous Phase:

$$\kappa(\mathcal{D}_d/\mathcal{D}_c)\, Pe^{-1/2} \gg 4 \times 10^{-2}. \tag{20}$$

The high value of solute distribution constant κ assures the simultaneous satisfaction of these two inequalities.

Most of the correlations developed in the literature have the Sherwood number as a function of the drop translational velocity. It is difficult to estimate the drop velocity accurately in a turbulent environment. Furthermore, except for Ruckenstein's (1964) cellular model and Yaron and Gal-Or's (1971) extension to multiparticulate swarms, all the equations are restricted to single drops. The contribution of a single drop to overall mass transfer in an aggregate of drops is not well understood. No investigation of the effects of one drop moving in the concentration wake of another and of spatial change in the concentration of the continuous phase associated with the dense dispersion has yet been reported.

The Schmidt number exponents of 1/3 and 1/2 represent the extremes of mass transfer mechanisms, namely, the slip velocity mechanism and the unsteady state theory, respectively. Depending on the interface mobility, in a given dispersion system, the exponent is likely to fall between these two extremes. Rowe et al. (1965) have indicated that the exponent for the Reynolds number increases from 0.4 to 0.6 as the Reynolds number increases. Levins and Glastonbury (1972) proposed a semiempirical correlation for mass transfer between the spherical solids and the stirred continuous phase.

$$Sh = 2 + 0.47(a^{4/3}\epsilon^{1/3}/\nu)^{0.62}(d/D_T)^{0.17}Sc^{0.36} \tag{21}$$

Hsia (1981) has shown that this corresponds to the Reynolds number exponent of 0.42, which lies toward the lower end of the range established by Rowe and coworkers. The Schmidt number exponent of 0.36 suggests that the mass transfer occurs by both mechanisms. However, its proximity to 0.33 suggests that the mass transfer occurs predominantly by the boundary layer mechanism.

TABLE 1. DISPERSION PHYSICAL PROPERTIES AT 298.15 K

Liquid	Density* ρ, kg/m^3	Viscosity** μ, Pa·s	Interfacial Tension† σ, N/m
Water	997	0.00090	—
Cyclohexane	770	—	0.0468
Carbontetrachloride	1,589	—	0.0480
Cyclohexane-Carbontetrachloride mixture	970	0.00082	0.0471
Molecular diffus. of iodine in water‡		1.0×10^{-9} m^2/s	
Partition coeff. of iodine between dispersed organic phase and continuous aqueous phase		62.17	

---

* Measured by the Chain Gravitometric Balance.

** Measured by the Brookfield Micro-Viscometer.

† Measured by the DuNuoy Tensiometer.

‡ Order of Magnitude value extrapolated from the data of Edgar and Diggs (1916) and Gregory and Riddiford (1956).

In a CFSTR, this applies to smaller drops whose interface mobility is considerably reduced as the drop size decreases. Iodine is used as the mass transfer solute in this work. As has been reconfirmed in this study, the nonsurface-active nature of iodine does not contribute to interface mobility due to the Marangoni effects. This factor stresses the need for the Schmidt number exponent to be near 0.33 in correlating iodine interface transfer. This aspect of iodine surface activity will be discussed later in this paper. Equation 21 is valid for mass transfer in both directions between the dispersed and the continuous phases with mass transfer resistance restricted to the continuous phase. The high partition coefficient of iodine ($\kappa = 62.17$) assures the satisfaction of the inequalities, Eqs. 19 and 20, under all experimental conditions of this investigation.

The considerations described above and the desire for simplicity dictated the use of Levins and Glastonbury correlation (Eq. 21) in *this investigation* to estimate iodine mass transfer between the dispersed and the continuous phases.

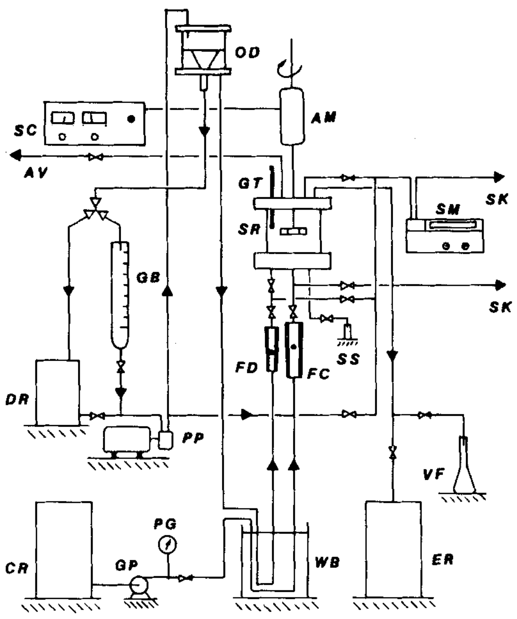

Figure 1. Experimental flow system.

AM:	**stirrer motor**	**OD:**	**overhead overflow device**
AV:	**vacuum line**	**PG:**	**pressure gauge**
CR:	**continuous phase feed reservoir**	**PP:**	**perstaltic pump for dispersed phase feed**
DR:	**dispersed phase feed reservoir**	**SC:**	**stirrer speed controller**
ER:	**effluent reservoir**	**SK:**	**sink line**
FC:	**continuous phase flowmeter**	**SM:**	**spectrophotometer**
FD:	**dispersed phase flowmeter**	**SR:**	**continuous flow stirred tank reactor**
GB:	**graduated buret for dispersed phase flow measurement**	**SS:**	**sampling station**
GP:	**continuous phase feed gear pump**	**VF:**	**volumetric flash for dispersion flow rate**
GT:	**mercury-in-glass thermometer**	**WB:**	**water bath**

EXPERIMENTAL SYSTEM

Choice of Experimental Dispersion

The exclusion of hydrodynamic flow patterns from this investigation imposes the restriction of homogeneous dispersion. This restriction requires a small difference in density and a high interfacial tension between the two immiscible phases of dispersion. Mutual solubility and solute-solvent interaction should also be at minimum to facilitate the thermodynamic, kinetic, and transport analysis. Accordingly, the system chosen was single distilled water as the continuous phase and a cyclohexane/carbontetrachloride mixture as the dispersed phase with iodine as the solute. The physical properties of the dispersion are given in Table 1. Quantitative analysis of iodine was carried out with a Beckman DB UV-VIS spectrophotometer. Iodine concentrations in the aqueous and organic phases were monitored at the absorption maxima of 460 and 524 nm, respectively. The molar absorptivity of the organic phase for which Beer's law was followed was 1,017.0 L/gmol·cm. Considerable deviation from Beer's law was observed for the continuous aqueous phase. The iodine concentration was correlated by the following fourth degree polynomial in absorbance.

$$C_c = (3.8133A - 1.4805A^2 + 1.6501A^3 - 0.5892A^4) \times 10^{-4}M \quad (22)$$

Experimental Apparatus

The experimental apparatus was designed for simultaneous data acquisition of mass transfer efficiency and drop size distribution in a two-phase liquid-liquid CFSTR. The experimental assembly consisted of two systems, namely, the flow system and the optical system.

Flow System. Figure 1 is a diagram of the experimental flow system. The two constituent phases of the liquid dispersion are continuously fed to a stirred tank *SR*, which is a cylindrical pyrex glass shell of 100 mm internal diameter sealed at the two ends by 303 austenitic stainless steel plates 102 mm apart. The reactor has four equally spaced glass baffles fused to the wall and a central six-blade Rushton turbine of 51 mm diameter. The turbine is driven by a motor *AM* (Ultra Masterflex Drive System, Cole Parmer Instruments Co.) which is regulated by a speed controller *SC*. The reactor is also equipped with a mercury-in-glass thermometer *GT*.

The estimation of mass transfer efficiency requires the measurement of solute concentration in either one of the two phases of the dispersion in the reactor. Being an optical densitometer instrument, a spectrophotometer cannot be used with liquid dispersions. A new technique of instantaneous phase separation by in situ membrane filtration was developed (Bapat, 1982; Bapat and Tavlarides, 1983). The aqueous phase filtrate was collected in the spectrophotometric cell (40 mm path length) at the sampling station *SS* in Figure 1. The iodine content of the separated organic phase can be continuously monitored by using a flow cell (1 mm path length) as shown in the Figure 1.

Optical System. A photomicrographic technique was developed to obtain the drop size distribution in the dispersed phase (Figure 2). The microflash *MF* (EG & G, #549-11) used in this work achieves a peak intensity of 50 million candles in 0.5 μs and thus effectively freezes the droplet motion in the reactor *SR*. The flash was synchronized with the camera shutter by a flash driver *FD*. The camera (Honeywell Pentax H3V) was mounted without its lens and coupled to the microscope by a microscope adapter.

Drop diameters were measured by projecting the micrograph negatives (Kodak Plus-X 35 mm Pan Film, ASA 125) on the screen of a semiautomatic drop picture analyzer (MOP-3, Carl Zeiss, Inc.). The output from this machine was manually fed to a digital computer to get the necessary drop size distribution statistics.

RESULTS AND DISCUSSION

The predictions of drop size distribution and mass transfer efficiency provided by the simulation algorithm are functions of the

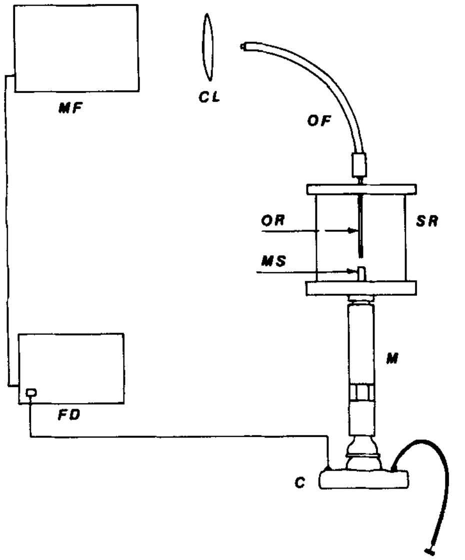

Figure 2. Optical system.

C: camera
CL: condensing lens
FD: microflash driver
M: microscope
MF: microflash
MS: microscope sleeve
OF: optical fiber
OR: optical rod
SR: stirred tank

drop rate processes. The breakage and coalescence frequencies used in this work (Eqs. 5 and 8, respectively) are functions of the physicochemical properties of the system but also involve four unknown constants, C_1, C_2, C_3, and C_4. Thus, the simulation predictions depend not only on the dispersion system and the operating conditions but also on the values assigned to these constants. By formulation of the droplet frequency functions, the constants are universal. Because of theoretical and experimental limitations, however, such a set of constants has not yet been found (Cruz-Pinto and Korchinsky, 1981). Table 2 gives the sets of constants used by Hsia (1981) in his simulation models to predict the drop size distributions for dispersions used by different workers. Although the sets vary for different workers, a definite region of application has been established. Trial-and-error search in and around this four-dimensional region was conducted to obtain a set of constants for use in this work. Since the constants are contained only in the frequency functions for breakage and coalescence, the search was carried out for steady state batch operation without mass transfer. Elimination of the reactor feed and effluent streams made the search more sensitive and efficient. Figure 3 shows the excellent agreement between the experimental and the simulated drop size distribution obtained by using the constants given in Table 2. The same set of constants has been used for all other predictions in this investigation.

Influence of Dispersed Phase Hold-up

Simulated and experimental variations of the dispersed phase Sauter diameter and extraction efficiency against the dispersed phase holdup are shown in the Figure 4. The results indicate that the Sauter mean diameter and the mass transfer efficiency increase with increasing phase fraction.

TABLE 2. BREAKAGE AND COALESCENCE CONSTANTS

Investigator	C_1	C_2	C_3 cm^{-3}	C_4 cm^{-2}
Hsia* (1981)	0.01031	0.06354	4.5×10^{-4}	1.891×10^9
Coulaloglou* (1975)	0.00487	0.0552	2.17×10^{-4}	2.28×10^9
Ross et al.* (1978)	0.00487	0.08	2.17×10^{-4}	3.0×10^8
This work	0.00481	0.08	1.9×10^{-3}	2.0×10^8

* As used by Hsia (1981).

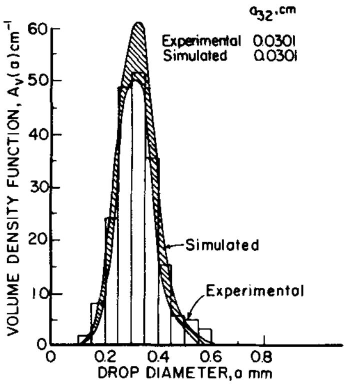

Figure 3. Experimental and simulated drop size distribution for physical dispersion: batch operation, 400 rpm; $\phi = 0.10$.

The increase in drop size is attributed to two mechanisms. With an increase in the dispersed phase fraction, the impeller energy per unit volume of the dispersed phase in the reactor decreases. This causes a reduction in the turbulent energy available for breakage *vis-a-vis* the drop surface energy. The damping effect of the higher phase fraction therefore leads to a larger drop size at a given agitator speed (Van Heuvan and Beek, 1971; Brown and Pitt, 1972; Doulah, 1975). The increased phase fraction also causes an increase in the collision frequency per unit volume of the dispersion. The increase in the drop size due to the increased phase fraction has been attributed to enhanced coalescence by Mlynek and Resnick (1972). Delichatsios and Probstein (1976) proposed that the increased drop size with higher fractional holdup can primarily be accounted for by coalescence, with turbulence damping playing a secondary role. The two mechanisms are adequately represented in this work by the drop and sample frequency functions (Eqs. 5–6, 8–10). The close agreement between the simulated and the experimental results in Figure 4 indicates that both the mechanisms contribute to the effect of dispersed phase holdup on the drop size.

The enhancement in the extraction efficiency is also the result of the greater crowding of the dispersed phase drops per unit volume of the reactor. The increased proximity of the drops promotes drop interactions which in turn promote interphase solute transfer. The enhancement in extraction efficiency is caused by the polydispersed nature of the dispersion. For a given concentration driving force, smaller drops lose their solute at a greater rate than larger drops. For example, according to the Levins and Glastonbury correlation used in this work (Eq. 21), the mass transfer coefficient is inversely proportional to the drop diameter raised to 0.173. In a weakly interactive dispersion, the solute concentrations in smaller drops are depleted with time and the overall concentration driving force operates the solute transfer at a deaccelerated rate. However, on mixing resulting from the drop interactions, the solute concentrations of the smaller drops are substantially increased as a

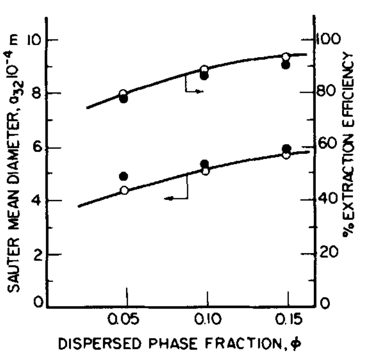

Figure 4. Influence of dispersed phase fraction on CFSTR performance at 350 rpm: τ = 60 s; $C_{d,f} = 1 \times 10^{-3}$ M; $C_{c,f}$ = ;0. ○: experimental; ●: simulated.

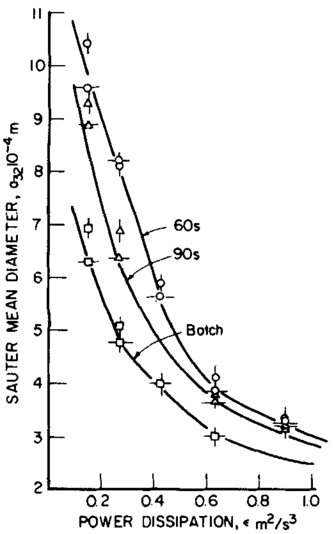

Figure 5. Influence of residence time on CFSTR drop size for physical dispersion: $\phi = 0.10$. O, 60 s; Δ, 90 s; □, batch; – –, experimental; |:, simulated.

result of the concentration averaging with the larger drops of higher concentrations. Drop interactions of coalescence and redispersion therefore place the solute in drops which are more efficient in interphase transport. It may be noted that the extraction efficiency shows an increasing trend with higher phase fraction in spite of the opposite effect generated by the turbulence damping.

Influence of Residence Time

Figure 5 shows the variation of Sauter mean diameter in relation to the rate of energy dissipation for physical dispersions for different residence times. Each point represents a residence time and the type of the result, either experimental or simulated. Superposition of experimental and simulated results has occured in some cases.

The figure shows that as the residence time increases, the Sauter mean diameter decreases. This result is characteristic of a dispersion that is dominated by breakage. In a CFSTR, for a given set of physicochemical properties the relative importance of breakage and coalescence is determined by the dispersed phase feed drop size. In the present work, the feed drop size is larger than the maximum drop size expected in the reactor under given operating conditions. Therefore, as soon as the drop enters it is subjected to breakage. With high residence time, drops are subjected to more breakage and thus the average drop size decreases. The batch operation provides the lower limit of average drop size as shown in Figure 5.

Figure 6 shows the variation of Sauter mean diameter and extraction efficiency with residence time for a stirrer speed of 350 rpm and a dispersed phase fraction of 0.10. The figure shows excellent agreement between the simulated and the experimental Sauter mean diameters. The simulated extraction efficiencies exceed the experimental values by nearly 6%.

Influence of Mass Transfer Direction

To ascertain the influence of mass transfer direction on the extractor performance, experiments were conducted with iodine transferring to and from the dispersed organic phase. Experiments were also conducted with physically and chemically equilibrated aqueous and organic feeds. The results (Figure 7) show that the Sauter mean diameters for the physically and chemically equilibrated dispersions are the same. Both dispersions are characterized by the absence of mass transfer, in the former because of the absence of solute and in the latter because of zero potential gradient.

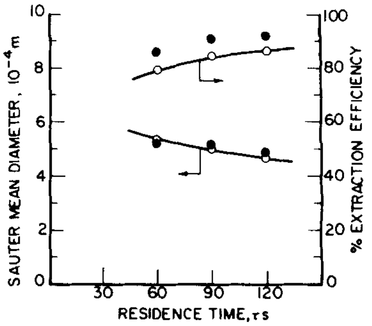

Figure 6. Drop size and efficiency versus residence time at 350 rpm: $\phi = 0.10$; $C_{d,f} = 1 \times 10^{-3}$ M; $C_{c,f} = 0$. O: experimental; ●: simulated.

The drop size for the dispersion in which iodine is transferred from the dispersed to the continuous phase is greater than for the dispersions without mass transfer. The drop size for reverse mass transfer is the same as without mass transfer. The data indicate that the mass transfer from the dispersed to the continuous phase increases the coalescence and the increased drop size causes a reduction in mass transfer efficiency. The mass transfer efficiency for reverse mass transfer is higher by virtue of its smaller drop size. A solute which reduces the interfacial tension between the two immiscible liquids, on transferring from the dispersed to the continuous phase, promotes coalescence (Johnson and Bliss, 1946; Groothuis and Zuiderweg, 1960). The closely related data of Khemangkorn et al. (1978) indicate that iodine reduces the interfacial tension between the aqueous and organic phases. The interfacial tension between carbontetrachloride and water decreased from 0.0445 to 0.0433 N/m when the aqueous iodine concentration increased from 5.8×10^{-4} M to 1.1×10^{-3} M. The interfacial tension without iodine was reported as 0.045 N/m. This reduction in interfacial tension promotes coalescence as iodine transfers from the dispersed to the continuous phase.

The effect of iodine interphase transfer on coalescence, however, is very small because of the weak surface activity of iodine. To increase the concentration gradients between the two phases, experiments were conducted with dispersed phase iodine feed concentration raised from 1×10^{-3} M (level 1) to 2×10^{-3} M (level 2) and 3×10^{-3} M (level 3). Similarly, for the reverse mass transfer, the continuous aqueous phase iodine feed concentration was raised from 1×10^{-4} M (level 1) to 2×10^{-4} M (level 2). No change in the interfacial gradients occurred, however, as evidenced by the absence of any significant variation in the average drop size and the extraction efficiency. The experimental data given in Table 3 show that the Sauter mean diameter and the extraction efficiency remain unchanged as the continuous phase iodine feed concentration is increased for the reverse mass transfer. Figure 7 also indicates that

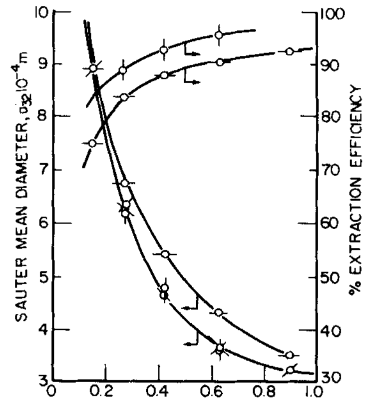

Figure 7. Influence of mass transfer direction on CFSTR performance. All data points are experimental. $\phi = 0.10$; $\tau = 90$ s; feed concentration level 1. ⌀: dispersion without solute; ⊂: dispersion with solute in equilibrium; -O-: solute transfer, d → c; ϕ: solute transfer, c → d.

TABLE 3. EFFECT OF SOLUTE FEED CONCENTRATION
Residence time 90 s. Dispersed phase hold-up fraction 0.10.

Direction of Transfer*	RPM	Sauter Mean Diameter, a_{32} (μm)		
		Level 1	Level 2	Level 3
(d → c)	250	889 (75.0)**	894 (80.0)	850 (78.1)
(d → c)	300	675 (83.9)	714 (88.2)	697 (87.8)
(d → d)	350	543 (87.8)	531 (90.9)	511 (90.4)
(d → c)	400	431 (90.3)	— (94.6)	— (95.1)
(d → c)	450	350 (92.3)	— (96.3)	— (94.9)
(c → d)	300	618 (88.9)	616 (88.3)	
(c → d)	350	475 (92.8)	468 (92.5)	
(c → d)	400	358 (95.2)	377 (94.1)	

---

* (d → c) denotes transfer from the dispersed to the continuous phase; (c → d) denotes transfer in the reverse direction.

** Number in the bracket following the sauter mean diameter is the percent extraction efficiency.

the solute mass transfer from the continuous phase to the dispersed phase does not cause a significant reduction in coalescence and that the Sauter mean diameters are almost equal to the dispersions without mass transfer.

Similar observations were made by Thornton and Pratt (1953) who studied the flooding rates in rotary annular columns. With acetone transferring from the dispersed organic solvent to the continuous aqueous phase, the flooding rates increased two to three times. For mass transfer in the reverse direction, the limiting throughput was only 10% lower than the limit observed without mass transfer. The effect was ascribed to the greater rising velocity and the lower holdup resulting from the considerably larger drops in the column when acetone was transferred from the dispersed to the continuous phase. No appreciable change in the drop size was noted when the transfer took place in the opposite direction.

In view of the relatively low surface activity of iodine compared to that of acetone, the absence of experimentally noticeable reduction in the average drop size in case of iodine transfer from the continuous to the dispersed phase appears plausible.

A quantitative analysis of liquid dispersions on the basis of a functional relationship between the solute concentration and the interfacial flow and their effect on coalescence frequency has not yet been attempted. Until this coupled problem of mass transfer in coalescing drop population is solved, the above experimental observations on the influence of mass transfer directions cannot be interpreted with rigor. For future experimental investigations of the effect of solute concentration and mass transfer direction, it is suggested that the solute be capable of significanlty altering the interfacial tension between the two immiscible phases of the dispersion.

ACKNOWLEDGMENT

This research was financed by the National Science Foundation Grant CPE-80-21039.

NOTATION

a = drop diameter, m
A = spectrophotometric absorption, Eq. 22
$A_v(a)$ = probability volume density function of a drop of diameter a, m^{-1}
B = birth rate of drops, s^{-1}
C = solute concentration, M or mol/m^3
C_1,C_2 = constants in the breakage frequency function, Eq. 5
C_3,C_4 = constants in the coalescence frequency function, Eq. 8
d = stirrer diameter, m
D = death rate of drops, s^{-1}
D_T = tank diameter, m
$\mathcal{D}$ = solute molecular diffusivity, m^2/s
E = reactor mass transfer efficiency
f_b = sample breakage frequency, s^{-1}
f_c = sample coalescence frequency, s^{-1}
f_e = sample exit frequency, s^{-1}
f_f = sample feed frequency, s^{-1}
$f_{c,i}$ = coalescence frequency of the drop diameter a_i, s^{-1}
$F(a_i,a_j)$ = coalescence frequency between drops of diameters a_i and a_j, s^{-1}
$g(a)$ = breakage frequency of a drop of diameter a, s^{-1}
k = mass transfer coefficient (based on the continuous phase), m/s
K = proportionality constant in Eq. 18
m_i = solute moles exchanged by the ith drop in the time interval t, moles
n = drop number density function, Eq. 1
N = total number of drops in the sample or population
Pe = Peclet number
Q = volumetric liquid flow rate, m^3/s
Re = Reynolds number
Sc = Schmidt number
Sh = Sherwood number
t = time, s
t_{IQ} = interval of quiescence, s
u = interfacial velocity at the drop equator, m/s
U = drop translational velocity, m/s
v_f = average volume of the feed drop, m^3
V = sample phase volume, m^3
x = uniform random number between 0 and 1
x = drop property vector

Greek Letters

$\beta(a_i;a_j)$ = probability density function of a daughter drop of diameter a_i when a drop of diameter a_j breaks
ϵ = power dissipation per unit mass, m^2/s^3
κ = solute equilibrium distribution constant, $C_{d,e}/C_{c,e}$
μ = dynamic viscosity, kg/m·s
ν = kinematic viscosity, m^2/s
ϕ = dispersed phase holdup fraction
ρ = density, kg/m^3
σ = interfacial tension, N/m
τ = residence time, s

Subscripts

c = continuous phase
d = dispersed phase
e = equilibrium
f = feed
1,2 = values before and after the interval of quiescence

Superscript

$*$ = initial value

LITERATURE CITED

Bajpai, R. K., D. Ramkrishna, and A. Prokop, "A Coalescence Redispersion Model for Drop Size Distributions in an Agitated Vessel," *Chem. Eng. Sci.*, **31**, 913 (1976).

Bapat, P. M., "Mass Transfer in a Liquid-Liquid Continuous Flow Stirred Tank Reactor," Ph.D. Thesis, Ill. Inst. Tech., Chicago, IL (1982).

Bapat, P. M., L. L. Tavlarides, and G. W. Smith, "Monte Carlo Simulation of Mass Transfer in Liquid-Liquid Dispersions," *Chem. Eng. Sci.*, **38**, 2003 (1983).

Bapat, P. M., and L. L. Tavlarides, "Phase Separation Technique for Liquid Dispersions," *Ind. Eng. Chem. Fund.*, **23**, 120 (1984).

Bayens, C. A., and R. L. Laurence, "A Model for Mass Transfer in a Coalescing Dispersion," *Ind. Eng. Chem. Fund.*, **8**, 71 (1969).

Boussnesq, J., "Calcul du pouvoir refroidissant des courants fluides," *J. Math. Pures Appl.*, **6**, 285 (1905).

Brown, D. E., and K. Pitt, "Drop Size Distribution of Stirred Non-Coalescing Liquid-Liquid System," *Chem. Eng. Sci.*, **27**, 577 (1972).

Clift, R., J. R. Grace, and M. E. Weber, *Bubbles, Drops and Particles*, Academic Press, New York (1978).

Coulaloglou, C. A., "Dispersed Phase Interactions in an Agitated Flow Vessel," Ph.D. Thesis, Ill. Inst. Tech., Chicago, IL (1975).

Coulaloglou, C. A., and L. L. Tavlarides, "Description of Interaction Processes in Agitated Liquid-Liquid Dispersions," *Chem. Eng. Sci.*, **32**, 1289 (1977).

Cruz-Pinto, J. J. C., and W. J. Korchinsky, "Drop Breakage in Counter Current Flow Liquid-Liquid Extraction Columns," *Chem. Eng. Sci.*, **36**, 687 (1981).

Curl, R. L., "Dispersed Phase Mixing. I: Theory and Effects in Simple Reactors," *AIChE J*, **9**, 175 (1963).

Dang, V., E. Ruckenstein, and W. N. Gill, "Quasi-Steady State Assumption for Mass Transfer to Spherical Binary Bubbles or Drops," *The Chem. Eng.*, **241**, 248 (1970).

Delichatsios, M. A., and R. F. Probstein, "The Effect of Coalescence on the Average Drop Size in Liquid-Liquid Dispersions," *Ind. Eng. Chem. Fund.*, **15**, 134 (1976).

Doulah, M. S., "An Effect of Hold-Up on Drop Sizes in Liquid-Liquid Dispersions," *Ind. Eng. Chem. Fund.*, **14**, 137 (1975).

Edgar, G., and S. H. Diggs, "The Diffusion of Iodine in Potassium Iodide Solutions," *J. Am. Chem. Soc.*, **38**, 253 (1916).

Gordon, G., *System Simulation*, 2nd ed., Prentice Hall, Englewood Cliffs, NJ (1969).

Graybeal, W. J., and U. W. Pooch, *Simulation: Principles and Methods*, Winthrop Pub., Cambridge, MA (1980).

Gregory, D. P., and A. C. Riddiford, "Transport to the Surface of a Rotating Disc," *J. Chem. Soc.*, 3,756 (1956).

Groothuis, H., and F. J. Zuiderwag, "Influence of Mass Transfer on Coalescence of Drops," *Chem. Eng. Sci.*, **12**, 288 (1960).

Hsia, M. A., "The Modeling of Liquid-Liquid Extraction in Stirred Tanks by a Simulation Approach," Ph.D. Thesis, Ill. Inst. Tech., Chicago, IL (1981).

Hsia, M. A., and L. L. Tavlarides, "A Simulation Model for Homogeneous Dispersions In Stirred Tanks," *Chem. Eng. J.*, **20**, 225 (1980).

———, "Simulation Analysis of Drop Breakage, Coalescence and Micromixing in Liquid-Liquid Stirred Tanks," *Chem. Eng. J.*, **26**, 189 (1983).

Jakubowsky, S., and S. Sideman, "A Simulation Model for Two- and Three-Phase Agitated Systems," *Int. J. Multiphase Flow*, **3**, 171 (1976).

Johnson, H. F., and H. Bliss, "Liquid-Liquid Extraction in Spray Towers," *Trans. Am. Inst. Chem. Eng.*, **42**, 331 (1946).

Khemangkorn, V., J. Molinier, and H. Angelino, "Influence of Mass Transfer Direction on Efficiency of a Pulsed Perforated Plate Column," *Chem. Eng. Sci.*, **33**, 501 (1978).

Levins, D. M., and J. R. Glastonbury, "Particle-Liquid Hydrodynamics and Mass Transfer in a Stirred Vessel. II: Mass Transfer," *Trans. Inst. Chem. Eng.*, **50**, 132 (1972).

Mlynek, Y., and W. Resnick, "Drop Sizes in an Agitated Liquid-Liquid System," *AIChE J.*, **18**, 122 (1972).

Ramkrishna, D., "Drop Breakage in Agitated Liquid-Liquid Dispersions," *Chem. Eng. Sci.*, **29**, 987 (1974).

Randolph, A. D., and M. A. Larson, *Theory of Particulate Processes Analysis and Techniques of Continuous Crystallization*, Academic Press, New York, (1971).

Ross, S. L., F. H. Verhoff, and R. L. Curl, "Droplet Breakage and Coalescence Processes in an Agitated Dispersion. 2: Measurement and Interpretation of Mixing Experiments," *Ind. Eng. Chem. Fund.*, **17**, 101 (1978).

Rowe, P. N., K. T. Claxton, and J. B. Lewis, "Heat and Mass Transfer from a Single Sphere in an Extensive Flowing Fluid," *Trans. Inst. Chem. Eng.*, **43**, T14 (1965).

Ruckenstein, E., "On Mass Transfer in the Continuous Phase from Spherical Bubbles or Drops," *Chem. Eng. Sci.*, **19**, 131 (1964).

———, "Mass Transfer between a Single Drop and a Continuous Phase," *Int. J. Heat Mass Transfer*, **10**, 1,785 (1967).

———, "A Generalized Penetration Theory for Unsteady Convective Mass Transfer," *Chem. Eng. Sci.*, **23**, 363 (1968).

Shah, B. H., D. Ramkrishna, and J. D. Borwanker, "Simulation of Particulate Systems using the Concept of the Interval of Quiescence," *AIChE J.*, **23**, 897 (1977).

Skelland, A. H. P., *Diffusional Mass Transfer*, John Wiley & Sons, New York (1974).

Spielman, L. A., and O. Levenspiel, "A Monte Carlo Treatment for Reacting and Coalescing Dispersed Phase Systems," *Chem. Eng. Sci.*, **20**, 247 (1965).

Thornton, J. D., and H. R. C. Pratt, "Liquid-Liquid Extraction. VII: Flooding Rates and Mass Transfer Data for Rotary Annular Columns," *Trans. Inst. Chem. Eng.*, **31**, 289 (1953).

Valentas, K. J., and N. R. Amundson, "Breakage and Coalescence in Dispersed Phase Systems," *Ind. Eng. Chem. Fund.*, **5**, 533 (1966).

Van Heuvan, J. W., and W. J. Beek, "Power Input, Drop Size and Minimum Stirrer Speed for Liquid-Liquid Dispersion in Stirred Vessels," *Proc. ISEC*, **1**, 70, Amsterdam (1971).

Yaron, I., and B. Gal-Or, "Convective Mass or Heat Transfer from Size-Distributed Drops, Bubbles or Solid Particles," *Int. J. Heat Mass Transfer*, **14**, 727 (1971).

Zeitlin, M. A., and L. L. Tavlarides, "Fluid-Fluid Interactions and Hydrodynamics in Agitated Dispersions: A Simulation Model," *Can. J. Chem. Eng.*, **50**, 207 (1972).

Manuscript received Jan. 20, 1983; revision received Oct. 11, 1983, and accepted Jan. 3, 1984.